

# A Robust Velocity Field Control

Ilse Cervantes, Rafael Kelly, Jose Alvarez-Ramirez, and Javier Moreno

**Abstract**—This paper is devoted to velocity field control (VFC) of uncertain robotic manipulators. We propose a proportional-integral (PI)-type controller derived from modeling error compensation ideas and singular perturbation theory, that requires a minimum knowledge of the plant (i.e., constant estimate of the inertia matrix). It is shown that semiglobal practical stabilization is achieved; that is, given any compact set of initial velocity field errors, there exist PI control gains which guarantee that the robot tracks a desired velocity field with arbitrary accuracy. The proposed controller was experimentally evaluated on a two degrees-of-freedom arm.

**Index Terms**—Integral control, semiglobal stability, uncertain robot dynamics, velocity field control (VFC).

## I. INTRODUCTION

OVER the past 20 years, there has been a great deal of research in the field of robot path planning and control. Much of this work has been focused on finding the most appropriate way to represent robot actions during a navigation task or during a machining operation. Notwithstanding, the more common way of representing the robot actions is through a desired timed trajectory. In this way, motion control—or also called tracking control—of robot manipulators has been defined by using a timed trajectory in order to reproduce the desired motion. The motion control algorithm guarantees asymptotic tracking of the desired trajectory. Motion control problem is well studied in, e.g., [1] and [2].

Velocity field control (VFC) has emerged recently from the literature [3], [4] as alternative to motion control. VFC approach proposes to encode the robot actions through a velocity field; that is, a velocity tangent vector is defined at every point of the configuration space [3].

Many useful robotic tasks, such as following contour tasks for machining operation like cutting, milling, and deburring, can be effectively encoded through a velocity field. This approach has several advantages over the traditional trajectory tracking.

- 1) The velocity field error is a more appropriate way to describe whether the contour is being followed.
- 2) The specification of the task, encoded as vector field, and the speed at which the task is performed can be decoupled [4].

Manuscript received January 18, 2001. Manuscript received in final form February 5, 2002. This work was supported in part by CONACYT under Grant 32613-A. Recommended by Associate Editor K. Kozłowski.

I. Cervantes is with SEPI-ESIME Culhuacan, Instituto Politecnico Nacional, Col. San Francisco Culhuacan, Mexico City, D.F. 04430, Mexico (e-mail: ilse@calmecac.esimecu.ipn.mx).

R. Kelly and J. Moreno are with the Division de Fisica Aplicada, CICESE, Ensenada, B.C. 22800, Mexico.

J. Alvarez-Ramirez is with the Division de Ciencias Basicas e Ingenieria, Universidad Autonoma Metropolitana-Iztapalapa, Mexico City, D.F. 09340, Mexico.

Digital Object Identifier 10.1109/TCST.2002.804126

- 3) The coordination aspect of the task is explicit [5].

By specifying a contour task using a velocity field the robot is guided toward the contour in the most expedient manner based on its current location. On the other hand, situations arise in which a timed trajectory based controller tries to catch up with the desired timed trajectory, and leaves the desired contour in the process. This causes a phenomenon known as radial reduction in which the actual path traced out has a smaller radius than the one specified by desired trajectory. The velocity field approach to contour following is able to trade off time keeping in favor of coordination [5].

On the other hand, several applications of the velocity field approach has been reported, e.g., teleoperated manipulators [6], cooperative multiple manipulators systems [7], cooperative multiple mobile robots [8] and adaptive passive velocity field control [9]. However, there are several questions that remain open, e.g., regarding the velocity field control of uncertain robot systems. This paper works along these lines. We propose a proportional-integral (PI)-type controller, which requires a minimum knowledge of the plant (e.g., constant estimate of the inertia matrix). It is shown that, given any initial condition in position and velocity joints, the desired velocity field can be tracked with arbitrary accuracy (semiglobal practical stability).

*Notation:* Throughout this paper,  $|\cdot|$  stands for the Euclidean norm of a vector,  $\|\cdot\|$  stands for the induced norm,  $I_n$  is the  $n$ -dimensional identity matrix, and  $\lambda_{\min}\{A\}$ ,  $\lambda_{\max}\{A\}$  denotes, respectively, the minimum and maximum eigenvalue of a positive definite matrix  $A$ .  $0_n$  denotes the origin of  $\mathbb{R}^n$ .  $Dh(x)$  denotes the derivative of  $h$  with respect to  $x$  and  $\otimes$  denotes Kronecker product (see [1] for definition).

## II. MODEL DESCRIPTION AND CONTROL PROBLEM FORMULATION

Consider the general equations describing the dynamics of a  $n$ -degrees-of-freedom robot manipulator

$$M(q)\ddot{q} + C(q, \dot{q})\dot{q} + g(q) = \tau \quad (1)$$

where  $q \in \mathbb{R}^n$  is the vector of joint displacements,  $\tau \in \mathbb{R}^n$  is the vector of applied joint torque inputs,  $M(q) \in \mathbb{R}^{n \times n}$  is the symmetric positive-definite manipulator inertia matrix,  $C(q, \dot{q}) \dot{q} \in \mathbb{R}^n$  is the vector of centripetal and Coriolis torques, and  $g(q) \in \mathbb{R}^n$  is the vector of gravitational torques.

Following the notation introduced in [4], let  $T_q\mathcal{G}$  be the tangent space of  $\mathcal{G}$  at a specific manipulator configuration  $q$ , where  $\mathcal{G}$  is a  $n$ -dimensional configuration manifold. A time-invariant desired velocity field is a map

$$\begin{aligned} \vartheta: \mathcal{G} &\rightarrow T\mathcal{G}, \\ q &\mapsto \vartheta(q) \in T_q\mathcal{G} \end{aligned}$$

where  $T\mathcal{G} = \bigcup_{q \in \mathcal{G}} T_q\mathcal{G}$  is the tangent bundle of  $\mathcal{G}$ . Thus, the desired velocity field defines a tangent vector at every point  $q$  of the configuration space

$$\dot{q} = \vartheta(q).$$

The VFC problem can be stated as that of designing a torque input  $\tau$  in such a way that the actual joint velocity  $\dot{q}$  reaches the prescribed velocity field  $\vartheta(q)$ , i.e.,

$$\lim_{t \rightarrow \infty} [\vartheta(q(t)) - \dot{q}(t)] = 0. \quad (2)$$

The VFC problem is addressed under the following assumptions.

- A.1) The functions  $M(q)$ ,  $C(q, \dot{q})$  and  $g(q)$  are uncertain and  $C^1$ -functions.
- A.2) The velocity field  $\vartheta(q)$  has continuous bounded first- and second-time derivatives.
- A.3) The velocity field  $\vartheta(q)$  yields uniformly globally bounded trajectories [i.e.,  $\|q(0) + \int_0^t \vartheta(q(\sigma)) d\sigma\|$  is globally bounded for all  $q(0) \in \mathbb{R}^n$  and  $t \geq 0$ ].

### III. VFC: EXACT FEEDBACK DESIGN

In this section, we address the VFC control problem by assuming that the robot model and parameters are known. The purpose is twofold: 1) to introduce a basic constructive step toward the design of robust control design and 2) to assess the limit of what can be attained with such controller.

Let  $v = \dot{q}$  be the robot velocity, and let  $e_r \stackrel{\text{def}}{=} \vartheta(q) - v \in \mathbb{R}^n$  be the velocity field error. The robot dynamics (1) can be written as

$$\begin{aligned} \dot{q} &= \vartheta(q) - e_r \\ \dot{e}_r &= \beta(q, e_r) - M(q)^{-1}[\tau - \varphi(q, e_r)] \end{aligned} \quad (3)$$

where

$$\beta(q, e_r) \stackrel{\text{def}}{=} D\vartheta(q)[\vartheta(q) - e_r] \in \mathbb{R}^n$$

and

$$\varphi(q, e_r) \stackrel{\text{def}}{=} g(q) + C(q, (\vartheta(q) - e_r))[\vartheta(q) - e_r] \in \mathbb{R}^n.$$

The inverse-dynamics feedback controller

$$\tau = F_1^{\text{inv}}(q, e_r) \stackrel{\text{def}}{=} \varphi(q, e_r) + M(q)[\beta(q, e_r) + K_r e_r] \quad (4)$$

where  $K_r \in \mathbb{R}^{n \times n}$  is a positive-definite matrix, yields

$$\begin{aligned} \dot{q} &= \vartheta(q) - e_r \\ \dot{e}_r &= -K_r e_r \end{aligned} \quad (5)$$

so that  $\lim_{t \rightarrow \infty} e_r(t) = 0$  exponentially and, by virtue of Assumption A.3,  $q(t)$  remains bounded for all  $t \geq 0$ .

*Remark 1:* If  $R(q)$  is the  $\omega$ -limit set of the trajectories generated by the vector field  $\vartheta(q)$  [i.e.,  $q(0) + \int_0^t \vartheta(q(\sigma)) d\sigma \rightarrow R(q(t))$  asymptotically], then,  $R(q) \times 0_n$  is the  $\omega$ -limit set of the system (5). Notice that, by virtue of Assumption A.3,  $R(q) \times 0_n$  is a compact set.

*Remark 2:* Basically, VFC is a cascade or backstepping control configuration [10]. In fact, the desired velocity field  $\vartheta(q)$

is designed on the basis of the relative-degree one system  $\dot{q} = v^*$ , where  $v^*$  is taken as a virtual control input. In this way, the so-called primary or master control loop is  $v^* = \vartheta(q)$ . Since the actual system is  $\dot{q} = v$ , the action of the master loop yields  $\dot{q} = \vartheta(q) - e_r$ . In this way, the aim of the secondary or slave control loop is to achieve zero velocity tracking error [i.e.,  $\lim_{t \rightarrow \infty} e_r(t) = 0$ ]. This objective is attained via the inverse dynamics feedback  $\tau = F_1^{\text{inv}}(q, e_r)$ . As mentioned in the introduction, the advantage of a cascade control configuration over its noncascade counterpart is that the specification of the task, encoded as a vector field, and the speed at which the task is performed can be decoupled [4].

*Remark 3:* It is interesting to consider the case when  $\vartheta(q) = K_\vartheta(q_d - q)$ , where  $K_\vartheta$  is a positive-definite matrix, and  $q_d \in \mathbb{R}^n$  is a desired position. In this case, the point  $R(q) = q_d$  becomes the  $\omega$ -limit set of the vector field  $K_\vartheta(q_d - q)$ . Since  $D\vartheta(q) = -K_\vartheta$ , the corresponding inverse-dynamics feedback controller is

$$\tau = \varphi(q, e_r) - M(q)[-K_1(q_d - q) + K_2 v] \quad (6)$$

where  $K_1 = K_r K_\vartheta$  and  $K_2 = K_r + K_\vartheta$ . The controller (6) is the well-known computed torque control, which stabilizes the system about the desired robot position  $q_d$ .

### IV. VFC: ROBUST FEEDBACK DESIGN

The inverse-dynamics control law (4) ensures that the robot system (1) tracks the desired velocity field asymptotically. Unfortunately, given that the robot model is uncertain, this control law cannot be implemented. To avoid this problem, an inverse-dynamics robust controller will be designed later.

Let  $\bar{\varphi}(q, e_r)$  be an estimate of the function  $\varphi(q, e_r)$  defined as

$$\bar{\varphi}(q, e_r) = \bar{g}(q) + \bar{C}(q, \vartheta(q) - e_r)(\vartheta(q) - e_r)$$

where  $\bar{g}(q)$  and  $\bar{C}(q, \vartheta(q) - e_r)$  are the estimates of gravity and Coriolis torques, respectively. A modeling error function, say  $\eta(q, e_r, \tau)$ , can be defined as follows:

$$\eta(q, e_r, \tau) \stackrel{\text{def}}{=} -M(q)^{-1}[\tau - \varphi(q, e_r)] + \bar{M}(q)^{-1}[\tau - \bar{\varphi}(q, e_r)] \quad (7)$$

where  $\bar{M}(q)$  is a positive-definite matrix estimate of the inertia matrix  $M(q)$ . In this way, the system (3) can be rewritten as

$$\begin{aligned} \dot{q} &= \vartheta(q) - e_r \\ \dot{e}_r &= \beta(q, e_r) + \eta(q, e_r, \tau) - \bar{M}(q)^{-1}[\tau - \bar{\varphi}(q, e_r)]. \end{aligned} \quad (8)$$

In terms of the modeling error function  $\eta(q, e_r, \tau)$ , the inverse-dynamics controller (4) becomes

$$\begin{aligned} \tau &= F_2^{\text{inv}}(q, e_r, \eta(q, e_r, \tau)) \\ &\stackrel{\text{def}}{=} \bar{\varphi}(q, e_r) + \bar{M}(q)[\beta(q, e_r) + \eta(q, e_r, \tau)] + \bar{M}(q)K_r e_r. \end{aligned} \quad (9)$$

*Remark 4:* The inverse-dynamics feedback function  $\tau = F_2^{\text{inv}}(q, e_r, \eta(q, e_r, \tau))$  is an implicit representation

of the exact feedback function  $\tau = F_1^{\text{inv}}(q, e_r)$ . In fact,  $F_1^{\text{inv}}(q, e_r) = F_2^{\text{inv}}(q, e_r, \eta(q, e_r, F_1^{\text{inv}}(q, e_r)))$ .

Following modeling error compensation ideas [11], and owing to the fact that

$$\eta(q, e_r, \tau) = \dot{e}_r - \beta(q, e_r) + \overline{M}(q)^{-1}[\tau - \overline{\varphi}(q, e_r)]$$

the signal<sup>1</sup>  $\eta(t) = \eta(q(t), e_r(t), \tau(t))$  can be reconstructed using the following reduced-order observer:

$$\begin{aligned} \dot{\overline{\eta}} &= \xi^{-1}[\eta - \overline{\eta}] \\ &= \xi^{-1}[\dot{e}_r - \beta(q, e_r) + \overline{M}(q)^{-1}[\tau - \overline{\varphi}(q, e_r)] - \overline{\eta}] \end{aligned} \quad (10)$$

where  $\overline{\eta} \in \mathbb{R}^n$  is the estimate of  $\eta(t)$  and  $\xi^{-1} > 0$  is the observer gain. Based on this observation, our choice of practical controller is the certainty-equivalence feedback corresponding to (9)

$$\tau = F_2^{\text{inv}}(q, e_r, \overline{\eta}) \quad (11)$$

where the uncertain term  $\eta(q, e_r, \tau)$  of the inverse-dynamics control law (9), has been replaced by the estimate  $\overline{\eta}$ . The resulting robust controller is composed by the modeling error estimator (12) and the certainty-equivalence feedback function (11).

*Remark 5:* The observer (10) is improper since it requires the time-derivative  $\dot{e}_r$ . By introducing the variable  $w \stackrel{\text{def}}{=} \xi \overline{\eta} - e_r$ , this observer can be easily implemented. In this way, we get the proper estimator

$$\begin{aligned} \dot{w} &= -\beta(q, e_r) + \overline{M}(q)^{-1}[\tau - \overline{\varphi}(q, e_r)] - \xi^{-1}(w + e_r) \\ \overline{\eta} &= \xi^{-1}(w + e_r) \end{aligned} \quad (12)$$

with initial condition  $w(0) = \xi \overline{\eta}(0) - e_r$ , if  $\overline{\eta}(0)$  is taken as zero then  $w(0) = -e_r(0)$ .

*Remark 6:* It is not difficult to see that the practical controller (11), (12) can be rewritten as follows:

$$\tau = P(q, \dot{q}) + \overline{M}(q)F_{PI}(e_r) \quad (13)$$

where

$$P(q, \dot{q}) = \overline{M}(q)\beta(q, e_r) + \overline{\varphi}(q, e_r) \quad (14)$$

and

$$F_{PI}(e_r) = K_P e_r + K_I \int_0^t e_r(\sigma) d\sigma$$

is a classical linear PI controller with gains

$$\begin{aligned} K_P &= \xi^{-1}I_n + K_r \\ K_I &= \xi^{-1}K_r. \end{aligned} \quad (15)$$

Notice that when  $\overline{C}(q, \dot{q})$  and  $\overline{M}(q)$  are chosen as diagonal (constant) matrices, (13) becomes a decentralized control composed by a linear PI control plus a velocity field dynamics compensator. Furthermore, if the velocity field is given as in Remark 3, the controller (13) becomes a classical proportional-integral-derivative (PID) controller with derivative gain  $K_D = \overline{M}K_\vartheta$ .

<sup>1</sup>By some abuse of notation, the symbol  $\eta$  was used to denote both the signal  $\eta(t)$  and the function  $\eta(q(t), e_r(t), \tau(t))$ .

*Remark 7:* The practical control (11), (12) is an exact observed-based representation of inverse-dynamics control with integral action [12]. This representation has several advantages over its traditional counterpart. For instance, anti-reset windup schemes to cope with actuator saturations can be easily introduced [12]. In Section V, we will exploit the exact observer-based representation (11), (12) to describe the closed-loop system as a singularly perturbed system.

## V. STABILITY ANALYSIS

In this section, we study the closed-loop stability of the candidate practical VFC, yielding a robust stability condition coupled with a systematic tuning procedure.

### A. Closed-Loop Equations

To simplify computations, let us take  $\overline{M}(q)$  as a constant matrix and  $\overline{\varphi}(q, e_r) = 0$ . Denote the observation error as

$$e_\eta \stackrel{\text{def}}{=} \eta - \overline{\eta} \in \mathbb{R}^n.$$

By using (11) in (8), we get the controlled robot dynamics

$$\begin{aligned} \dot{q} &= \vartheta(q) - e_r \\ \dot{e}_r &= -K_r e_r + e_\eta. \end{aligned} \quad (16)$$

On the other hand, by virtue of (10), the dynamics of the estimation error becomes

$$\dot{e}_\eta = -\xi^{-1}e_\eta + \dot{\eta}. \quad (17)$$

It is possible to compute the time-derivative  $\dot{\eta}$  from (7), (10), and (11) to get

$$\dot{e}_\eta = -\xi^{-1}M^{-1}\overline{M}e_\eta + \Psi(q, e_r, e_\eta) \quad (18)$$

where

$$\begin{aligned} \Psi(q, e_r, e_\eta) &\stackrel{\text{def}}{=} -M^{-1}\overline{M} \left[ \dot{\beta}(q, e_r) + K_r e_\eta - K_r^2 e_r \right] \\ &\quad + M^{-1}\dot{\varphi}(q, e_r) + \dot{\beta}(q, e_r) + K_r e_\eta - K_r^2 e_r \\ &\quad + M^{-1}\dot{M}[\beta(q, e_r) - e_\eta + K_r e_r] \end{aligned} \quad (19)$$

and

$$\dot{M} = [[\vartheta(q) - e_r]^T \otimes I_n] [DM(q)],$$

### B. Main Stability Result

Summarizing, in the coordinates  $(q, e_r, e_\eta)$ , the closed-loop system can be written as

$$\begin{aligned} \dot{q} &= \vartheta(q) - e_r \\ \dot{e}_r &= -K_r e_r + e_\eta \\ \xi \dot{e}_\eta &= -M^{-1}\overline{M}e_\eta + \xi \Psi(q, e_r, e_\eta). \end{aligned} \quad (20)$$

For small values of  $\xi > 0$ , the system (20) becomes a singularly perturbed system. Since  $M^{-1}\overline{M}$  is an invertible matrix, the corresponding reduced system is

$$\begin{aligned} \dot{q} &= \vartheta(q) - e_r \\ \dot{e}_r &= -K_r e_r \end{aligned} \quad (21)$$

which is obtained by setting  $\xi = 0$  in (20). Notice that the reduced system is the closed-loop robot system under the exact inverse-dynamics controller [see (4)]. Hence, the reduced system (21) has globally exponentially convergence of the velocity error  $e_r(t)$  to zero, with globally bounded position trajectories  $q(t)$ . The boundary-layer system is obtained by taking a new time scale  $\chi = t/\xi$  in (20) and setting  $\xi = 0$ , that is

$$e'_\eta = -M^{-1}\overline{M}e_\eta \quad (22)$$

where  $e'_\eta = de_\eta/d(\chi)$ . Regarding the stability of system (22), we have the following result.

*Lemma 1:* Assume that  $\|M(q)^{-1}\overline{M} - I_n\| \leq \alpha < 1$ , for all  $q \in \mathbb{R}^n$  and some  $\alpha > 0$ . Then, the boundary-layer system (22) is uniformly exponentially stable about the origin.<sup>2</sup>

*Proof:* Write the boundary-layer system (22) as

$$e'_\eta = -[I_n - \Gamma(q)]e_\eta \quad (23)$$

where  $\Gamma(q) \stackrel{\text{def}}{=} I_n - M^{-1}\overline{M}$ . The time-derivative of the positive function  $V_{e_\eta} = e_\eta^T e_\eta$  along the trajectories of (23) satisfies  $V'_{e_\eta} = -2V_{e_\eta} + e_\eta^T[\Gamma(q) + \Gamma(q)^T]e_\eta \leq -2(1 - \alpha)V_{e_\eta} < 0$ , for  $V_{e_\eta} \neq 0$ . This shows that (23) is globally exponentially stable with Lyapunov function  $V_{e_\eta}(e_\eta) = e_\eta^T e_\eta$ . ■

The next result establishes the stability properties of system (20) for an arbitrary selection of the velocity field  $\vartheta(q)$ .

*Proposition 1:* The velocity field error of the closed-loop system (20) is semiglobally practically stable about the  $\omega$ -limit set  $R(q) \times 0_n$ . This is, for each compact set pair  $(B_{(q, e_r)}, W_{(q, e_r)})$ , neighborhoods of  $R(q) \times 0_n$ , with  $B_{(q, e_r)} \subset W_{(q, e_r)} \subset \mathbb{R}^{2n}$ , there exists a positive value  $\xi_{\max}$  and a pair of compact sets  $(B_{e_\eta}, W_{e_\eta})$ , neighborhoods of the origin with  $B_{e_\eta} \subset W_{e_\eta} \subset \mathbb{R}^n$ , such that all the solutions of the closed-loop system (20), with initial condition in  $W_{(q, e_r)} \times W_{e_\eta} \subset \mathbb{R}^{3n}$ , are captured by the set  $B_{(q, e_r)} \times B_{e_\eta} \subset \mathbb{R}^{3n}$ , for all  $0 < \xi < \xi_{\max}$ .

*Proof:* Once the closed-loop system has been described as a singularly perturbed system, the proof of the stability result follows as a direct application of the results in [13]. In fact, notice that by virtue of Assumption A.1,  $\Psi(q, e_r, e_\eta)$  has bounded derivatives on compact sets. Lemma 1 implies that the boundary-layer system is exponentially stable about the origin. Hence, [13, Th. 2] and matched asymptotic expansions solutions imply that, for  $t \geq 0$  and small  $\xi > 0$ , the solution of (20) with initial conditions in the compact set  $W_{(q, e_r)} \times W_{e_\eta} \subset \mathbb{R}^{3n}$  satisfies

$$\begin{aligned} q(t, \xi) &= q_0(t) + \xi \tilde{q}_1(t) + \mathcal{O}(\xi^2) \\ e_r(t, \xi) &= e_{r,0}(t) + \xi \tilde{e}_{r,1}(t) + \mathcal{O}(\xi^2) \\ e_\eta(t, \xi) &= e_{\eta,0}(t) + \xi \tilde{e}_{\eta,1}(t) + \mathcal{O}(\xi^2) \end{aligned}$$

where  $(q_0(t), e_{r,0}(t))$  and  $e_{\eta,0}(t)$  are, respectively, the solutions of the reduced and the boundary-layer systems,  $\tilde{q}_1(t)$ ,  $\tilde{e}_{r,1}(t)$  and  $\tilde{e}_{\eta,1}(t)$  are first-order terms in the matched asymptotic expansion of solutions. Hence, for small  $\xi > 0$ , the trajectories of system (20) converge to a neighborhood

<sup>2</sup>In [1], we see that there always exists a choice of  $\overline{M}$  satisfying such inequality.

$B_{(q, e_r)} \times B_{e_\eta} \subset \mathbb{R}^{3n}$  of the compact set  $R(q) \times 0_n \times 0_n$ . Moreover, such neighborhood is  $\mathcal{O}(\xi)$ . As a consequence, the  $\omega$ -limit set  $R(q) \times 0_n$  is semiglobally practically stable. ■

It can be shown that the result in Proposition 1 is also valid when  $\overline{\varphi}(q, e_r) \neq 0$  and the matrix  $\overline{M}$  is not constant. In fact, the proof can be made following the same steps made in the proof of Proposition 1, previous computation of the closed-loop dynamics.

*Remark 8:* Notice that

$$\begin{aligned} q(t, \xi) &\rightarrow q_0(t) \\ e_r(t, \xi) &\rightarrow e_{r,0}(t) \\ e_\eta(t, \xi) &\rightarrow e_{\eta,0}(t) \end{aligned}$$

uniformly as  $\xi \rightarrow 0$ . That is, the trajectories of the full singularly perturbed system (20) converge to the trajectories of the system composed by the reduced and the boundary-layer system. As a consequence, we conclude that as  $\xi \rightarrow 0$ , the robust VFC  $F_2^{\text{inv}}(q, e_r, \overline{\eta})$  [see (11)] recovers the performance induced by the exact VFC  $F_1^{\text{inv}}(q, e_r)$  [see (4)].

*Remark 9:* Since the coupling function  $\Psi(q, e_r, e_\eta)$  may not be globally Lipschitz, and hence has not globally bounded derivatives, due to the Coriolis/centripetal forces  $C(q, v)v$ , the initial conditions of the closed-loop system (20) are restricted to any given compact set. In turn, this leads to semiglobal stability results only.

*Remark 10:* The result in Proposition 1 states that, given any compact set of initial positions and velocity errors (semiglobal stability), there exist PI parameters which guarantee that the robot tracks the desired velocity field with arbitrary accuracy (practical stability). This is done by taking a sufficiently small value of the observer gain  $\xi > 0$ . Smaller  $\xi > \xi_{\max}$  leads to a larger set of initial conditions  $W_{(q, e_r)} \times W_{e_\eta}$  and a smaller residual tracking set  $B_{(q, e_r)} \times B_{e_\eta}$ .

*Remark 11 (Semiglobal Asymptotic Stability):* If the  $\omega$ -limit set of the vector field  $\vartheta(q)$  is a desired position, say  $q_d$  (see, for instance, Remark 3), then  $\Psi(q_d, 0, 0) = 0$ . In this case, the reduced system (21) has a asymptotic limit point  $(q_d, 0_n) \in \mathbb{R}^{2n}$ . Reference [13, Th. 3] implies that the equilibrium position  $(q_d, 0_n) \in \mathbb{R}^{2n}$  is semiglobally asymptotically stable. In addition, if  $\vartheta(q) = K_\vartheta(q_d - q)$ ,  $\overline{M}(q)$  is a constant positive-definite matrix, and  $\overline{C}(q, v) = 0$ ,  $F_2^{\text{inv}}(q, e_r, \overline{\eta})$  is equivalent to a classical linear PID controller (see Remark 6). Hence, Proposition 1 provides a theoretical support for the widely usage of linear PID control in the point-to-point regulation of robot manipulators.

### C. Bounded Input Control

From a practical point of view, it is interesting to analyze the case when the control input is subject to constraints. Given the torque bounds  $\tau_{\min}$  and  $\tau_{\max}$ , the robot system (1) under the exact feedback control law (4) is asymptotically stable and has a region of attraction  $\Omega \subseteq \mathbb{R}^{2n}$ . Under bounded control actions, the result of Proposition 1 implies the existence of PI parameters for which, the robot tracks the desired velocity field with arbitrary accuracy, provided that the set of initial position and velocity errors are contained in  $\Omega$  (semiglobal stability with respect to  $\Omega$ ). As in the unbounded input case, this is done by taking a sufficiently small value of the observer gain  $\xi > 0$ . That

is, smaller values of  $\xi$  implies that the actual region of attraction tends to  $\Omega$ , and smaller residual set.

Futhermore, the observer-based PI control representation (10), (11) has an important advantage over the standard PI representation: *it is equipped with an antireset windup (ARW) scheme*. In fact, if  $\tau^c$  is the computed torque (the controller output) and  $\tau^{\text{sat}} = \text{sat}(\tau^c)$  is the actual torque acting on the robot manipulator, where  $\text{sat}(\cdot)$  is a suitable saturation function, then the control law (10), (11) can be rewritten as

$$\tau = P(q, \dot{q}) + \bar{M}(q)F_{PI}(e_r) + G_{\text{ARW}} \int_0^t (\tau^{\text{sat}}(\sigma) - \tau^c(\sigma)) d\sigma$$

where  $G_{\text{ARW}}$  a gain matrix. The ARW scheme is given by the feedback signal  $G_{\text{ARW}}, \int_0^t (\tau^{\text{sat}} - \tau^c) d\sigma$ . In this way, when the control input is saturated (i.e.,  $\tau^{\text{sat}} - \tau^c \neq 0$ ), the above feedback signal tries to drive the ‘‘control input error’’  $\tau^{\text{sat}} - \tau^c$  to zero by recomputing the integral such that the control  $\tau^c$  attains exactly its saturation limit. This prevents the control loop from severe stability and performance degradation induced by integral action winding.

#### D. Tuning Guidelines

From Proposition 1, the  $\xi$ -parameterization (15) for  $0 < \xi < \xi_{\text{max}}$  defines a trajectory in the  $\{K_P, K_I\}$ -space for which practical stability of the controlled robot system is ensured. This fact and the previous stability analysis enable us to extract simple tuning guidelines which guarantee a stable implementation of the controller (13).

- 1) Choose  $\bar{M}$  to satisfy the condition of Lemma 1 (see [1]).
- 2) Choose the inner-loop matrix gain  $K_r$  according with a given performance criteria.
- 3) Choose a sufficiently small value of  $\xi > 0$  so as to get an acceptable closed-loop stability (Proposition 1). Compute the PI control gains with the identities (15).

Notice that  $\xi$  influences inversely the PI performance: the smaller the value of  $\xi > 0$ , the larger the estimate of the region of attraction  $W_{(q, e_r)} \times W_{e_\eta}$  and the smaller the residual set  $B_{(q, e_r)} \times B_{e_\eta}$ . Of course, in practice the minimum value of  $\xi > 0$  is limited by measurement noise and nonmodeled dynamics, e.g., actuator dynamics. In the following section, we will illustrate that good VFC performance can be attained with moderate values of  $\xi > 0$ .

## VI. EXPERIMENTAL EVALUATION

This section is devoted to show the experimental evaluation of the proposed robust VFC on a two-degrees-of-freedom arm. A complete description of the robot and its parameters can be found in [14] and [15]. For completeness in presentation, a brief outline of the experimental implementation is given later.

The robot consists of two links made of 6061 aluminum both actuated by brushless direct drive servo actuator to drive the joints without gear reduction. The motors used in the robot manipulator are the DM1200-A and DM1015-B models from Parker Compumotor for the shoulder and elbow joints, respectively. The servos are operated in torque mode, so the motors act as torque source and they accept an analog voltage

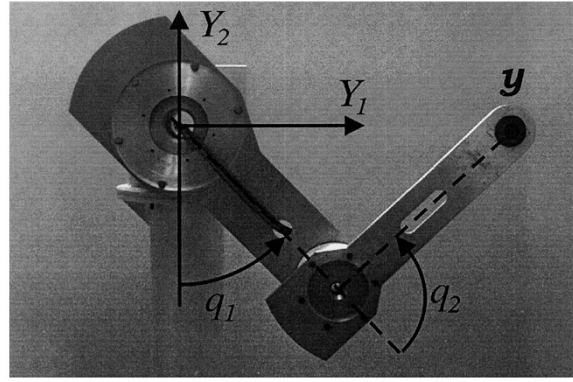


Fig. 1. Experimental setup.

as a reference of torque signal. In this configuration the motor DM1200-A is capable to deliver 200 Nm torque output and the motor DM1015-B only 15 Nm.

Position information is obtained from incremental encoders located on the motors, which have a resolution of 1 024 000 p/r for the first motor and 655 360 p/r for the second one. The accuracy for both motors is 30 arc/s. A motion control board based on a TMS320C31 32-bit floating point microprocessor from Texas Instruments, is used to execute in a PC Pentium II host computer.

A vector field with a circular contour in task coordinates as a ( $\omega$ -limit) global attractor was chosen. The origin of the Cartesian frame is attached at the axis of rotation of the fist joint, while  $y_1$  and  $y_2$  denote the horizontal and vertical axes, respectively (see Fig. 1). The vector field was chosen to exhibit a behavior without abrupt changes in velocity and acceleration such that saturation of actuators were prevented. The mathematical expression of the desired velocity field is

$$\nu(y) = -k(y)f(y) \begin{bmatrix} 2(y_1 - y_{c1}) \\ 2(y_2 - y_{c2}) \end{bmatrix} + c(y) \begin{bmatrix} -2(y_2 - y_{c2}) \\ 2(y_1 - y_{c1}) \end{bmatrix} \quad (28)$$

where

$$f(y) = (y_1 - y_{c1})^2 + (y_2 - y_{c2})^2 - r_0^2$$

$$k(y) = \frac{k_0^*}{|f(y)| \|\nabla f(y)\| + \epsilon}$$

$$c(y) = \frac{c_0 \exp^{-\mu|f(y)|}}{\|\nabla f(y)\|}$$

$r_0 = 0.2$  m is the circle diameter,  $y_{c1} = 0.318$  m and  $y_{c2} = 0.318$  m defines the circle center coordinates,  $k_0^* = 0.1 \text{ ms}^{-1}$ ,  $\mu = 20 \text{ m}^{-2}$ ,  $\epsilon = 0.005 \text{ m}^3$ , and  $c_0 = 0.1 \text{ ms}^{-1}$  is the desired tracking speed.

Since the controller proposed in this paper was designed to track a desired velocity field in joint coordinates, a previous step has to be made, in order to translate the velocity field from Cartesian to joint coordinates. To this end, we use the direct kinematics of the robot

$$y = \begin{bmatrix} l_1 \sin(q_1) + l_2 \sin(q_2 + q_1) \\ -l_1 \cos(q_1) - l_2 \cos(q_1 + q_2) \end{bmatrix}.$$

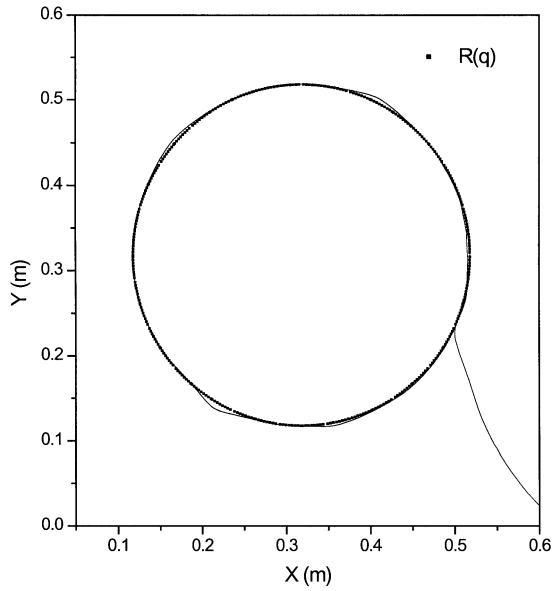


Fig. 2. Experimental traced contour.

Then, the analytical Jacobian is given by

$$J(q) = \begin{bmatrix} l_1 \cos(q_1) + l_2 \cos(q_1 + q_2) & l_2 \cos(q_1 + q_2) \\ l_1 \sin(q_1) + l_2 \sin(q_1 + q_2) & l_2 \sin(q_1 + q_2) \end{bmatrix} \quad (29)$$

where  $l_1$  and  $l_2$  are, respectively, the length of the first and second links. The desired velocity field in joint coordinates is then given by  $\vartheta(q) = J(q)^{-1}v(y)$ .

The objective of the experimental evaluation is two fold. First, to illustrate that the task of choosing an estimate of inertia matrix  $\bar{M}$  satisfying Lemma 1, does not constitute a difficult one. Second, to illustrate the performance of the proposed controller. To this end, we have chosen  $\bar{M} = \text{diag}(3.0, 0.2)$ , whose elements are upperbounds of the diagonal elements of  $M(q)$ . The inner loop gain matrix was  $K_r = \text{diag}(6.6, 6.6) \text{ Nm s rad}^{-1}$ . The initial conditions were  $q_1(0) = 45 \text{ deg}$ ,  $q_2(0) = 90 \text{ deg}$  [i.e.,  $y(0) = (0.636, 0)^T \text{ m}$  in Cartesian coordinates],  $\dot{q}_1(0) = 0 \text{ rad s}^{-1}$  and  $\dot{q}_2(0) = 0 \text{ rad s}^{-1}$ . The link velocities were computed via backward differentiation with sampling period of 2.5 ms.

Fig. 2 shows the contour traced by the arm tip in comparison to that in reference for an observer gain  $\xi = 0.025 \text{ s}^{-1}$ . On the other hand, Figs. 3 and 4 present the time evolution of velocity field errors for three different values of the observer gain  $\xi$  (i.e.,  $\xi = 0.025 \text{ s}^{-1}$ ,  $\xi = 0.050 \text{ s}^{-1}$ ,  $\xi = 0.080 \text{ s}^{-1}$ ). It can be observed that smaller the value of  $\xi$ , the smaller the asymptotic velocity field tracking error (practical stability).

## VII. CONCLUSION

In this paper, we studied the velocity field control of robot manipulator in joint coordinates via a PI-type control. This controller is based on modeling error compensation techniques, so a minimum knowledge of the robot system is required. (That is, a constant estimate of the inertia matrix.) It is shown that semiglobal practical stabilization is achieved; that is, given any compact set of initial velocity field errors, there exist PI control gains which guarantee that the robot tracks a desired velocity

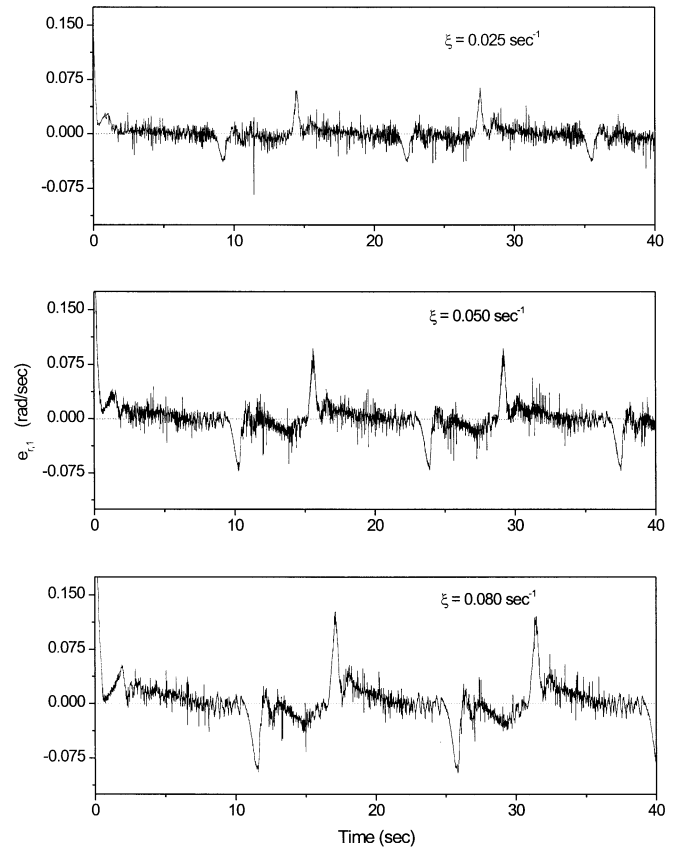


Fig. 3. Time evolution of the velocity field error for the first link.

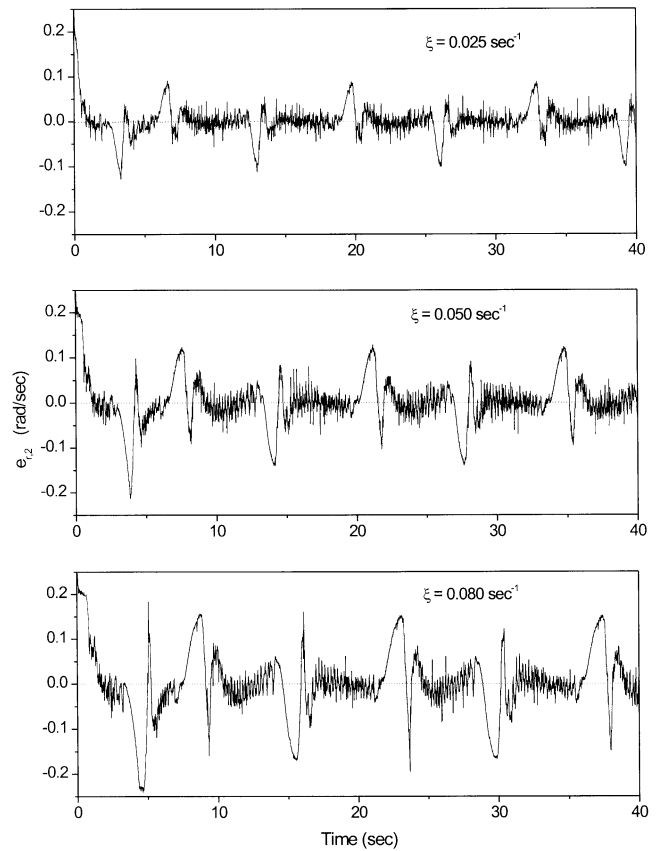


Fig. 4. Time evolution of the velocity field error for the second link.

field with arbitrary accuracy. Experimental work on a two-link robot arm was carried out to illustrate the performance and to assess the robustness of the proposed control.

- [15] —, “Experimental evaluation of model-based controllers on a direct-drive robot arm,” *Mechatronics*, vol. 11, pp. 267–282, 2001.

#### REFERENCES

- [1] M. W. Spong and M. Vidyasagar, *Robot Dynamics and Control*. New York: Wiley, 1989.
- [2] L. Sciacivco and B. Siciliano, *Modeling and Control of Robot Manipulators*. New York: McGraw-Hill, 1996.
- [3] P. Y. Li and R. Horowitz, “Passive velocity field control of mechanical manipulators,” in *Proc. Int. Conf. Robotics Automat.*, Nagoya, Japan, May 1995, pp. 2764–2770.
- [4] —, “Passive velocity field control of mechanical manipulators,” *IEEE Trans. Robot. Automat.*, vol. 15, pp. 751–763, Aug. 1999.
- [5] J. Li and P. Y. Li, “Passive velocity field control (PVFC) approach to robot force control and contour following,” in *Proc. JUSAFSA*, Ann Arbor, MI, July 2000.
- [6] P. Y. Li, “Passive control of bilateral teleoperated manipulators,” in *Proc. Amer. Contr. Conf.*, Philadelphia, PA, June 1998.
- [7] M. Yamakita, K. Suzuki, X.-Z. Zheng, M. Katayama, and K. Ito, “An extension of pasive velocity field control to cooperative multiple manipulators systems,” in *Proc. IEEE Int. Conf. Intell. Robot. Syst.*, vol. 1, September 1997, pp. 11–16.
- [8] M. Yamakita, T. Yazawa, X.-Z. Zheng, and K. Ito, “An application of passive velocity field control to cooperative multiple 3-wheeled mobile robots,” in *Proc. IEEE Int. Conf. Intell. Robot. Syst.*, vol. 1, Oct. 1998, pp. 1368–1373.
- [9] P. Y. Li, “Coordinated contour following control for machining operations—A survey,” in *Proc. Amer. Contr. Conf.*, San Diego, CA, June 1999, pp. 4543–4547.
- [10] M. Krstic, I. Kanellakopoulos, and P. V. Kokotovic, *Nonlinear and Adaptive Control Design*. New York: Wiley, 1995.
- [11] J. Alvarez-Ramirez, “Adaptive control of feedback linearizable systems: A modeling error compensation approach,” *Int. J. Robust Nonlinear Contr.*, vol. 9, pp. 361–377, 1999.
- [12] D. Alazard and P. Apkarian, “Exact observer-based structures for arbitrary compensators,” *Int. J. Robust Nonlinear Contr.*, vol. 9, pp. 101–118, 1999.
- [13] F. Hoppensteadt, “Asymptotic stability in singular perturbation problems. II: Problem having matched asymptotic expansion solutions,” *J. Differential Equations*, vol. 15, pp. 510–521, 1974.
- [14] F. Reyes and R. Kelly, “Experimental evaluation of identification schemes on a direct drive robot,” *Robotica*, vol. 15, pp. 563–571, 1997.